Identification of Functionally Important Amino-Terminal Arginines of *Agrobacterium tumefaciens* ADP-Glucose Pyrophosphorylase by Alanine Scanning Mutagenesis†

Diego F. Gómez-Casati,‡ Robert Y. Igarashi,§,|| Christopher N. Berger,§,⊥ Mark E. Brandt,§ Alberto A. Iglesias,‡ and Christopher R. Meyer*,§

Department of Chemistry and Biochemistry, California State University, Fullerton, California 92834, and Instituto Tecnológico de Chascomús, P.O. Box 164, Chascomús 7130, Argentina

Received November 14, 2000; Revised Manuscript Received June 20, 2001

ABSTRACT: Treatment of the *Agrobacterium tumefaciens* ADP-glucose pyrophosphorylase with the arginyl reagent phenylglyoxal resulted in complete desensitization to fructose 6-phosphate (F6P) activation, and partial desensitization to pyruvate activation. The enzyme was protected from desensitization by ATP, F6P, pyruvate, and phosphate. Alignment studies revealed that this enzyme contains arginine residues in the amino-terminal region that are relatively conserved in similarly regulated ADP-glucose pyrophosphorylases. To functionally evaluate the role(s) of these arginines, alanine scanning mutagenesis was performed to generate the following enzymes: R5A, R11A, R22A, R25A, R32A, R33A, R45A, and R60A. All of the enzymes, except R60A, were successfully expressed and purified to near homogeneity. Both the R5A and R11A enzymes displayed desensitization to pyruvate, partial activation by F6P, and increased sensitivity to phosphate inhibition. Both the R22A and R25A enzymes exhibited reduced V_{max} values in the absence of activators, lower apparent affinities for ATP and F6P, and reduced sensitivities to phosphate. The presence of F6P restored R22A enzyme activity, while the R25A enzyme exhibited only ∼1.5% of the wild-type activity. The R32A enzyme displayed an ∼11.5-fold reduced affinity for F6P while exhibiting behavior identical to that of the wild type with respect to pyruvate activation. Both the R33A and R45A enzymes demonstrated a higher activity than the wild-type enzyme in the absence of activators, no response to F6P, partial activation by pyruvate, and desensitization to phosphate inhibition. These altered enzymes were also insensitive to phenylglyoxal. The data demonstrate unique functional roles for these arginines and the presence of separate subsites for the activators.

ADP-glucose pyrophosphorylase (ADPGlc PPase,[1] EC 2.7.7.27) catalyzes the conversion of Glc-1-P and ATP to ADP-glucose and pyrophosphate, which is a key regulated step in both bacterial glycogen and plant starch biosynthesis (*1*−*4*). As a major control point for the production of renewable and biodegradable carbon sources, ADPGlc PPase is an attractive enzyme target for protein engineering. ADPGlc PPase regulation is mediated by the binding and effect of various activators and inhibitors, depending on the carbon assimilation pathway of the organism. In general, typical bacterial ADPGlc PPases are activated by glycolytic intermediates and inhibited by AMP, ADP, and/or P_i, while the cyanobacterial and plant enzymes are activated by 3-PGA and inhibited by P_i (*1*−*4*). These allosteric modulators have been shown to affect both the V_{max} of the reaction and the $S_{0.5}$ values for the substrates (*1*−*4*).

Although bacterial ADPGlc PPases have been grouped into seven different classes based on activator specificity (*4*), only enzymes from two of the activator classes (represented by the *Escherichia coli* and *Anabaena* PCC 7120 enzymes) have been studied in any molecular detail. The major activator of the *E. coli* enzyme is FBP (*4*). Chemical modification and site-directed mutagenesis studies of the *E. coli* enzyme have provided evidence for the roles of Lys-39 (*1*, *3*, *4*), Lys-195 (*1*, *4*), and Tyr-114 (*4*) in the binding of the activator FBP, the substrate Glc-1-P, and the substrate ATP, respectively. The regions surrounding these positions are fairly conserved in both plant and bacterial ADPGlc PPases (*5*). A highly conserved glycine rich region has also been identified near the N-terminus [in *E. coli*, amino acids 25−30 (LAGGRG)] that has been predicted to be part of a loop that interacts with the phosphates of ATP (*1*). It has also been postulated that the *E. coli* enzyme, in accord with the allosteric model of Monod et al (*6*), exists in two conformations: a high-activity form (R state), triggered by the binding of substrates

† This work was supported in part by NSF RUI Grant MCB-9905234 and Research Corporation Grants CC4232 and CC5506 to C.R.M. A.A.I. and D.F.G.-C. were supported by CONICET and Grant ANPCyT (PICT'99 1-6074) to A.A.I. C.N.B. was supported by NSF REU Grant CHE-9732290.

* To whom correspondence should be addressed. Phone: (714) 278-4173. Fax: (714) 278-5316. E-mail: cmeyer@fullerton.edu.

‡ Instituto Tecnológico de Chascomús.

§ California State University.

|| Current address: Department of Chemistry and Biochemistry, Utah State University, Logan, UT 84322.

⊥ Current address: Department of Biochemistry, University of California, Riverside, CA 92521.

[1] Abbreviations: ADPGlc PPase, ADP-glucose pyrophosphorylase; BSA, bovine serum albumin; CD, circular dichroism; DTE, dithioerythreitol; DTT, dithiothreitol; FBP, fructose 1,6-bisphosphate; F6P, fructose 6-phosphate; Glc-1-P, glucose 1-phosphate; Mg^{2+}, magnesium chloride; PGO, phenylglyoxal; P_i, phosphate.

10.1021/bi002615e CCC: $20.00
Published on Web 08/03/2001

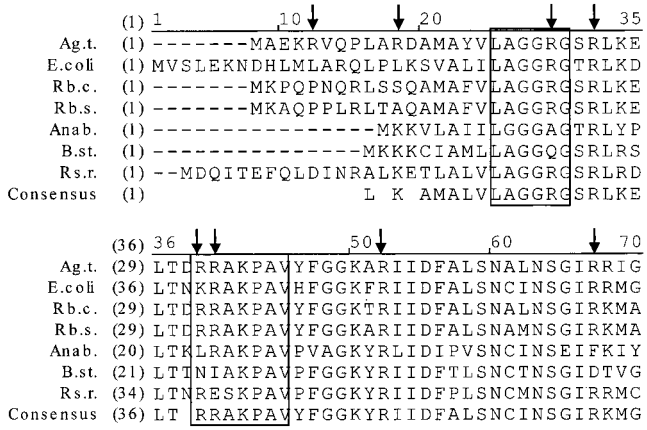

FIGURE 1: Comparison of the deduced amino acid sequences of the *A. tumefaciens* (Ag.t.) ADPGlc PPase N-terminus with other bacterial ADPGlc PPases. Multiple alignment (with identity boxes) of the N-terminal sequences from four different activator classes (*4*) represented by the sequences from *A. tumefaciens* (Ag.t.; *19*), *Rb. capsulatus* (Rb.c.; *14*), *Rb. sphaeroides* (*14*), *E. coli* (*4*), *Rs. rubrum* (Rs.r.; *14*), *B. stearothermophilus* (B.st.; *21*), and *Anabaena* PCC 7120 (Anab.; *17*). The arrows indicate the positions of arginine residues converted to alanine for analysis in the Ag.t. enzyme.

and activators, and a low-activity (T state) form favored by the binding of inhibitors (*7*).

Further studies have indicated the general importance of the N-terminus of ADPGlc PPase in the regulation of activity. In particular, the region beginning at Lys-39 in the *E. coli* enzyme [residues 39−45 (KRAKPAV)] has been shown to be important for activator binding or effect in a diverse number of ADPGlc PPases (*1*−*4*, *8*−*10*). Also, removal of the extreme N-terminus of the *E. coli* enzyme by both limited proteolysis (*11*) and truncation mutagenesis (*12*) was shown to result in an enzyme form that was both highly active in the absence of FBP and insensitive to inhibition by AMP.

Previous studies have probed the potential role of arginine(s) being involved in the binding of anionic substrate and effector molecules in various ADPGlc PPases (*13*−*18*). Further, arginine residues have been identified at or near highly conserved regions of the N-terminus (*13*, *14*). Although chemical modification experiments have indicated the importance of arginine residues in activity and regulation of ADPGlc PPase from *E. coli* (*15*), *Rhodobacter sphaeroides* (*13*), cyanobacteria (*16*, *17*), and spinach leaf (*18*), only one study has revealed the function of a specific arginine. An alanine scanning mutagenesis study of arginine residues conserved in plants and cyanobacteria (but not other bacteria) enzymes revealed that Arg-294 in the *Anabaena* PCC 7120 enzyme played a significant role in the binding of the inhibitor P_i (*17*).

Given the available data, it was of interest to obtain more information about the role of amino-terminal arginines in the activity and regulation of bacterial ADPGlc PPases. The recent cloning and expression of the ADPGlc PPase from *Agrobacterium tumefaciens* (*19*) has provided a valuable system for further exploring the amino acids responsible for regulation. This ADPGlc PPase is activated by F6P and pyruvate (*19*, *20*). Figure 1 displays an alignment of the N-terminal regions of selected bacterial ADPGlc PPases compared to the *A. tumefaciens* enzyme with arginine residues targeted for mutagenesis denoted with arrows. The enzyme from *Rhodobacter capsulatus* is activated by F6P and pyruvate (*20*). The enzyme from *R. sphaeroides* is activated by FBP, F6P, and pyruvate (*13*). The enzyme from *Rhodospirillum rubrum* is activated only by pyruvate (*4*). The *Bacillus stearothermophilus* enzyme is not significantly activated by any metabolite (*21*). The two boxed regions correspond to the highly conserved glycine rich region (*1*; in *A. tumefaciens*, amino acids 18−23) and the previously mentioned putative activator binding region. The *A. tumefaciens* enzyme has an arginine in place of the lysine found in the FBP-activated *E. coli* enzyme (RRAKPAV vs KRAKPAV), a difference shared by the enzymes from *Rb. sphaeroides* and *Rb. capsulatus* (*14*).

To successfully probe the role of N-terminal arginines, it was necessary to first obtain ample material for analysis by efficiently overexpressing the recombinant *A. tumefaciens* ADPGlc PPase gene and optimizing a purification scheme. Chemical modification of the purified recombinant enzyme with the arginyl reagent PGO resulted in desensitization to the activators F6P and pyruvate. Both the presence of the substrate ATP and the separate activators afforded protection from desensitization. Finally, this study, seminal in its examination of the N-terminal arginines of ADPGlc PPase, presents the effects of alanine substitution at the indicated positions (Figure 1).

EXPERIMENTAL PROCEDURES

Protein Sequence Alignment. The alignment of the amino-terminal bacterial ADPGlc PPase sequences (Figure 1) was performed using Clustal W (*22*) at the Biology WorkBench site and also with the AlignX module of VectorNTI (version 6.0, Informax Inc., North Bethesda, MD).

Subcloning and Expression of ADPGlc PPase. To increase the expression level of the *A. tumefaciens* enzyme, the *glgC* gene from pATUI (*19*) was subcloned into the pSE420 expression vector (Invitrogen). This vector utilizes the ATG included in the *Nco*I site as the start codon for heterologous protein expression. Due to an internal *Nco*I site in the coding region, the subcloning was performed as follows. (1) pSE420 was digested with *Nco*I, and the 5′ overhang was filled in with the Klenow fragment DNA polymerase followed by *Bgl*II digestion. (2) The coding region of ADPGlc PPase was PCR amplified from pATUI using a forward primer beginning with the first base of the second codon (5′-TCGGAAAAAAGAGTTCAG-3′) and a reverse primer (5′-GAAGATCTCTACAGGTCCAGCTTGTCGATCATC-3′) with an introduced *Bgl*II site (underlined). (3) The PCR product was digested with *Bgl*II and ligated into the digested pSE420 vector. The final construct (designated pBM472.4) was checked by restriction mapping and DNA sequencing and found to be free of PCR-introduced mutations in the coding region. The recombinant *A. tumefaciens* gene was expressed from pBM472.4 in TOP10 *E. coli* cells (grown in Terrific Broth) by induction of log phase cells ($OD_{600} \sim 0.5$) with 1 mM IPTG. The induced cells were harvested after ~18 h of growth at 37 °C by centrifugation at 2500*g* and stored frozen at −20 °C.

Site-Directed Mutagenesis. Site-directed mutagenesis was performed using the QuikChange kit (Stratagene). The following forward primers (and their complements) were used for conversion of arginine to alanine in the amino terminus (base changes are bold): R5A, 5′-ATG GCG GAA

AAA **GC**A GTT CAG CCT TTG-3′; R11A, 5′-CAG CCT TTG **GCA** GAT GCA ATG-3′; R22A, 5′-GTC GCA GGC GGA **GC**A GGA AGC CGT CTG AAG-3′; R25A, 5′-GGA AGA GGA AGC **GC**T CTG AAG GAA CTG AC-3′; R32A, 5′-GAA CTG ACG GAC **GC**C CGG GCA AAA CCC-3′; R33A, 5′-CTG ACG GAC CGC **GC**C GCA AAA CCC GCG GTT-3′; R45A, 5′-GGC GGC AAG GCG **GC**C ATC ATC GAT TTT-3′; and R60A, 5′-AAT TCC GGC ATC **GC**C CGC ATC GGC GTC-3′. The mutations and wild-type sequences were confirmed by DNA sequencing.

Purification of Recombinant Wild-Type and Altered ADPGlc PPases. All purification steps were carried out at 0−5 °C (unless noted). The presence of the enzyme was monitored in chromatography fractions by SDS−PAGE analysis (see *Gel Electrophoresis*) as enzyme activity is substantially inhibited by the presence of sulfate. After each step, the fractions containing the ∼50 kDa ADPGlc PPase subunit were pooled and concentrated using Centriprep-30 and Centricon-30 ultrafiltration concentrators (Amicon, Inc.). A 50 μL aliquot from each step was desalted into 50 mM glycine (pH 7.5) and 0.5 mM DTT using a P-6 Micro Bio-Spin column (Bio-Rad) to accurately determine the activity by the pyrophosphorolysis assay as described in *ADPGlc PPase Assay and Kinetic Analysis*. Protein concentrations were determined by the method of Bradford (*23*) using a kit from Bio-Rad with BSA as a standard. Cells harboring the expressed wild-type enzyme were resuspended (∼1 g of cells/2 mL) in a buffer containing 50 mM glycylglycine (pH 7.5), 5 mM DTT, and 1 mM EDTA, disrupted by sonication, and then centrifuged at 12000*g* to obtain soluble cell extracts. The crude extract was heat treated in a water bath set at 55 °C for 5 min, cooled on ice, and then centrifuged at 12000*g* for 15 min. Ammonium sulfate was added to 30% saturation to the supernatant and the precipitate removed by centrifugation at 12000*g* for 15 min. The supernatant was then diluted 2-fold with buffer A1 [50 mM glycine, 1.23 M ammonium sulfate, and 0.5 mM DTT (pH 7.5)] and loaded onto a Phenyl-Sepharose 6 (Fast Flow) column (2.5 cm × 8 cm, Pharmacia) equilibrated in the same buffer. After being washed with 3 column volumes of buffer A1, the column was subjected to a 0 to 48% buffer B1 [50 mM glycine and 0.5 mM DTT (pH 7.5)] gradient wash over 20 mL. The gradient was then held at 48% buffer B1 for 3 column volumes prior to enzyme elution with a 4 column volume gradient of 48 to 70% buffer B1. It should be noted that this step completely separates the small amount of endogenous *E. coli* ADPGlc PPase from the recombinant *A. tumefaciens* enzyme as the former elutes at nearly 100% buffer B1. The concentrated post-Phenyl-Sepharose fraction was then diluted 5-fold with buffer B1, and filtered (0.2 μm) prior to being loaded onto a UNO6 column (6 mL, Bio-Rad) attached to a BioLogic chromatography system (Bio-Rad). The enzyme was eluted from the column using the following procedure [buffer C1 included 50 mM glycine, 0.5 mM DTT, and 800 mM ammonium sulfate (pH 7.5)]. After being washed with 5 column volumes of buffer B1 followed by a 4 column volume wash with 5% buffer C1, the enzyme was eluted with a gradient of 5 to 75% buffer C1. The pooled enzyme fraction was desalted using a Bio-Rad Econo-Pac 10DG column into buffer D containing 50 mM glycine (pH 7.5), 2 mM Mg^{2+}, and 0.5 mM DTE, further concentrated to >1 mg/mL, and stored at −80 °C. The enzyme was found to be stable for at least 3 months. The enzyme was stored in small aliquots as repeated freeze−thaw cycles were found to result in some enzyme precipitation.

The altered enzymes, except for R60A, were purified as described for the wild-type enzyme except for the Phenyl-Sepharose step that was performed using an Econo-Pac column (10 mL bed, Bio-Rad). The washed column (in buffer A1) was eluted in 10 mL batches with 90, 80, 60, 45, 30, and 0% buffer A1. The enzyme typically eluted between 60 and 30% buffer A1. No significant activity could be measured for the R60A enzyme in the crude extract, although the level of total protein expression in the cells was comparable to those of the wild type and other altered enzymes. SDS−PAGE analysis indicated that proteolysis of the expressed protein may have occurred (data not shown). The R25A and R45A enzymes required the presence of 1 mM ATP with buffer D when frozen at −80 °C to remain stable; alternatively, these enzymes were stable for at least 1 week at 4 °C in the presence of 10% glyercol with buffer D.

Gel Electrophoresis. Denaturing gel electrophoresis was performed using 10% polyacrylamide/bisacrylamide (29:1) gels in the presence of 0.1% SDS as described by Laemmli (*24*) with the Bio-Rad Mini-Protean II system. Protein was detected by staining with Coomassie Brilliant Blue (R250, Sigma). Post-UNO6 wild-type and altered enzymes were found to be at least 95% homogeneous by SDS−PAGE.

ADPGlc PPase Assay and Kinetic Analysis. Enzyme assays performed in the pyrophosphorolysis direction (*25*) during purification included 80 mM Tris-HCl (pH 8.5), 0.5 mg/mL BSA, 8 mM Mg^{2+}, 10 mM NaF, 1 mM ADPGlc, 2 mM $^{32}PP_i$ (500−2000 cpm/nmol, NEN-DuPont), and 1.2 mM F6P in a final volume of 250 μL. Assays were performed at different enzyme concentrations to ensure steady-state conditions. The assays were initiated by the addition of enzyme [typically 0.001−0.1 μg in 10 μL freshly diluted in 50 mM HEPES (pH 7.5) with 1 mg/mL BSA and 0.5 mM DTE]. A unit of activity is defined as the amount of enzyme catalyzing the production of 1 μmol of [^{32}P]ATP per minute at 37 °C.

The highly pure post-UNO6 column enzyme was suitable for kinetic assays run in the ADPGlc synthesis direction (*26*). Assays were initiated with the addition of enzyme (in 10 μL, diluted as described above, yielding ∼2−20 nmol of product per assay). Depending on the protein concentration and assay conditions, we used typical enzyme dilutions ranging from 200- to 10000-fold. In all cases, enzyme dilutions assayed were in a linear range (enzyme concentration vs rate) during the time course of the assay. Data points typically represent the average of at least two determinations that differed by less than 6%. It should be noted that, as expected, the kinetic properties of the recombinant ADPGlc PPase were in good agreement with the previously published results (*19*; collected at pH 7.5). However, to better compare the data with previous studies on the similarly regulated enzymes from *Rb. capsulatus* (*20*) and *Rb. sphaeroides* (*13*), kinetic data were collected at pH 8. These results are in good general agreement with the data obtained at pH 7.5 (*19*). Small differences include ∼2- and 3-fold lower $S_{0.5}$ values for ATP (in the absence and presence of F6P, respectively) at pH 8 and no effect of F6P on the $S_{0.5}$ values for Glc-1-P and Mg^{2+} at pH 8.

Table 1: Purification of Recombinant *A. tumefaciens* ADPGlc PPase[a]

step	volume (mL)	[protein] (mg/mL)	protein (mg)	activity[b] (units)	specific activity (units/mg)	% yield	purification (*x*-fold)
sonication	30	22.2	666	6164	9.3	100	1
heat step	20	17.0	341	4499	13.2	73	1.4
ammonium sulfate	35	3.64	127	3401	26.7	55	2.9
Phenyl-Sepharose	90	0.46	41.4	2662	64.3	43	6.9
UNO6	0.4	18.9	7.58	1394	184	23	19.8

[a] Reported numbers are representative of an 8 g preparation from IPTG-induced *E. coli* TOP10 cells. [b] A unit of activity is defined here as the amount of enzyme producing 1 μmol of ATP per minute in the pyrophosphorolysis direction as indicated in Experimental Procedures.

Standard assays for activity measurements, in the ADP-glucose synthesis direction (*26*), included 100 mM HEPES-KOH (pH 8), 0.5 mg/mL BSA, 1 mM [^{14}C]Glc-1-P (1000−2000 cpm/nmol, NEN-DuPont), 5 mM Mg^{2+}, 2 mM ATP, 0.2 unit of inorganic pyrophosphatase (Sigma), and water in a total volume of 200 μL. Phosphate inhibition data were collected using standard conditions in the absence of any activators. Saturation plots for substrates and effectors were analyzed with the use of a computer program (*27*; using the Levenberg−Marquardt algorithm for regression) by fitting the data to the Hill equation. The resulting kinetic parameters were in very good agreement with those calculated from direct Hill plots. $S_{0.5}$, $A_{0.5}$, and $I_{0.5}$ are defined here as the concentrations of substrate, activator, and inhibitor that give 50% maximal activity, activation, and inhibition, respectively.

Chemical Modification with PGO. Prior to PGO modification, the enzyme (0.5 mg/mL) was desalted using a Bio-Spin column (as previously described) into a buffer containing 50 mM HEPES-KOH (pH 7.5). The reactions were initiated by the addition of PGO [solutions were freshly prepared in 50 mM HEPES-KOH (pH 7.5)], and the incubations were carried out at 25 °C. In all cases, enzyme activity and allosteric properties were stable under control conditions. Incubations were performed in the dark by wrapping the microfuge tubes in aluminum foil (to avoid photooxidation of other amino acids). At the indicated time points, aliquots were removed and added to an equal volume of stop buffer containing 100 mM HEPES-KOH (pH 7.5), 30 mM arginine, 1 mM DTT, and 1 mg/mL BSA to terminate the modification. The modified enzyme was assayed as indicated after appropriate dilution. The small carryover of arginine from the stop buffer had no effect on enzyme activity or response to effectors. The standard deviations (based on three to five measurements) for PGO modification activity data were typically between 2 and 5%. For protection studies, the reaction mixtures were supplemented with the desired ligand as indicated for 30 min in the presence and absence of 5 mM PGO. Preincubation with substrate and effector molecules did not result in any changes in activity or response to effectors.

Structural Characterization. To grossly assess the structural integrity of the mutant proteins, CD analysis was performed. CD spectra were obtained at 25 °C with a Jasco 720 CD spectropolarimeter. Samples (5−10 μM) of ADPGlc PPase (wild-type and mutants) in 20 mM Tris-HCl (pH 7.4) were placed in a cuvette with a 0.5 mm path length and data points obtained from 190 to 250 nm in 0.5 nm increments. The normalized spectra for wild-type and altered enzymes were essentially identical.

RESULTS

Expression and Purification of Wild-Type and Substituted Enzymes. Previous recombinant expression of the *A. tumefaciens* ADPGlc PPase in the older vector pKK223-3 (*28*) resulted in modest expression (specific activity ~3-fold higher than that from native *A. tumefaciens* in the crude extract; *19*). Further, the purification procedure involved three columns (DEAE, Phenyl-Superose, and MonoQ) and required a >700-fold purification to achieve near homogeneity. To more efficiently obtain the highly purified enzyme in amounts sufficient for functional studies, we subcloned the *glgC* gene into the newer expression vector pSE420 (Invitrogen) and optimized the purification protocol. Table 1 displays the purification of recombinant *A. tumefaciens* enzyme from 8 g of TOP10 cells. The specific activity of 9.3 units/mg present in the crude extract represents a >70-fold increase in expression level compared to that with the pKK223-3 vector (*19*) and is among the highest expression levels reported for a bacterial ADPGlc PPase. As described in Experimental Procedures, the removal of the DEAE chromatography step and the addition of an ammonium sulfate cut and Bio-Rad's UNO6 anion exchange column following Phenyl-Sepharose chromatography yielded a highly pure and active ADPGlc PPase. The final specific activity of 184 units/mg is the highest ever reported for this enzyme.

Chemical Modification of Wild-Type ADPGlc PPase with PGO. As previously mentioned, chemical modification of the *Rb. sphaeroides* ADPGlc PPase with both butanedione and PGO resulted in desensitization to the activators F6P, FBP, and pyruvate and the inhibitor P_i (*13*). To explore the potential role(s) of arginines in the *A. tumefaciens* enzyme, the effect of PGO modification was preliminarily examined. Treatment of the enzyme with 10 mM PGO for 60 min resulted in partial inactivation (to 60 ± 5% of the control rate in the absence of activators). Treatment with 5 mM PGO for 60 min resulted in a substantial loss in the level of activation by F6P (from 12- to 2.7-fold); an identical treatment with 10 mM PGO resulted in complete desensitization to F6P. The enzyme was partially desensitized to pyruvate activation by 5 and 10 mM PGO treatment (60 min) as the level of activation by pyruvate dropped from 8.5-fold to 4.0- and 2.7-fold, respectively. Treatment with 5 mM PGO for 30 min completely desensitized the enzyme to inhibition by 1 mM P_i (a concentration resulting in 50% inhibition of the control enzyme). A small but reproducible transient stimulation of activity was observed when the enzyme treated with 5 mM PGO was assayed in the absence of activators (the activity increased to 125 ± 5% of control) and in the presence of pyruvate (115 ± 5%) after a 15 min treatment. The inactivation of the F6P-stimulated activity was further

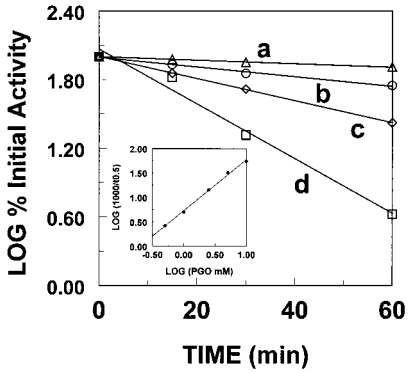

FIGURE 2: Effect of PGO on activation of *A. tumefaciens* ADPGlc PPase. Effect of PGO on activity measured in the presence of 2 mM F6P (log % initial activity) vs time in the presence of 1 (a), 2.5 (b), 5 (c), and 10 mM PGO (d). The inset displays the linear plot of log(1000/$t_{1/2}$) vs log[PGO] which also includes data from a 0.5 mM PGO time course.

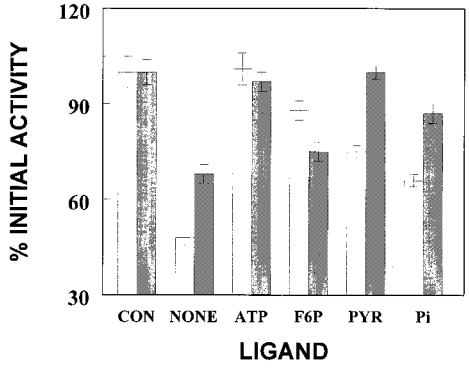

FIGURE 3: Protection by ligands of F6P-stimulated activity (left bars) and pyruvate-stimulated activity (right bars) from PGO. The reaction buffer was supplemented with the indicated ligand (2 mM) prior to treatment with 5 mM PGO for 30 min (see Materials and Methods). The initial specific activities of the controls (CON) were 147.9 ± 4.1 and 105.5 ± 5 units/mg for activity measured in the presence of 2 mM F6P and 2 mM pyruvate, respectively.

examined as shown in Figure 2. The observed inactivation is shown to be linear (following pseudo-first-order kinetics) in the semilog plot. The slope of the plot of log(1000/$t_{0.5}$) versus log(PGO) in the inset was linear (R value of 0.998) with a value of 1.05 indicating as few as one PGO molecule is required to modify the apparent F6P subsite.

These results, although not conclusive, are consistent with the presence of distinct functional arginine populations with differing sensitivities to PGO modification, potentially at allosteric and active site(s). Alternatively, modification of nonspecific arginine(s) could trigger indirect conformational changes resulting in the observed effects. In an attempt to distinguish between these possibilities, protection studies were performed as displayed in Figure 3. As expected, in the absence of any ligands (NONE), F6P-stimulated activity (left bar) was more sensitive to PGO than pyruvate-stimulated activity. The F6P-stimulated activity was well protected by ATP and F6P, while pyruvate and P_i were somewhat less effective. The pyruvate-stimulated activity (right bar) was most effectively protected by ATP and pyruvate, while F6P and P_i were less effective. The combination of 2 mM ATP and 5 mM Mg^{2+} gave equal protection to ATP alone, while Mg^{2+} alone afforded no protection (data not shown).

Site-Directed Mutagenesis of Amino-Terminal Arginines. Although the PGO modification data are supportive of functional roles for specific arginine residues at different subsites, such data provide no information about the exact arginine(s) involved. As previously indicated, amino-terminal arginines are likely to play functional roles in bacterial ADPGlc PPase activity and regulation. To meaningfully extend these data, the eight arginines in the first 60 amino acids of the N-terminus were converted to alanines by site-directed mutagenesis and the resulting substituted enzymes characterized. The multiple alignment shown in Figure 1 indicates the locations (with arrows) of arginines targeted for site-directed mutagenesis to alanine. These diverse arginines include two from the less conserved extreme N-terminus (R5 and R11), two associated with the conserved glycine rich region (R22 and R25), two that are part of the putative "activator binding site" (R32 and R33), and two highly conserved arginines further down the N-terminus in the primary sequence (R45 and R60). All of the altered enzymes, except the apparently unstable R60A, were successfully expressed and purified to near homogeneity. As described in Experimental Procedures, the near identical CD spectra as well as similar heat stability of the mutants compared to those of the wild-type enzyme indicate that these mutations did not grossly affect enzyme structure.

Effect of Mutations on the Kinetic Parameters for the Substrate ATP. Table 2 displays the kinetic parameters for the substrate ATP in the absence of effectors and in the presence of the activators F6P and pyruvate. All of the altered enzymes displayed essentially wild-type kinetics with respect to the substrate Glc-1-P and cofactor Mg^{2+} (data not shown).

In the absence of activators, the effects of the mutations on the apparent affinity for ATP, as assessed by the $S_{0.5}$ value, were modest, ranging from ~2- to 3.5-fold higher than the wild-type value. The R45A and R22A enzymes had the lowest apparent affinity for ATP, while the $S_{0.5}$ value for the R32A enzyme was essentially identical to the wild-type value. In contrast, more drastic V_{max} effects were observed. The R25A enzyme had ~0.25% of the wild-type activity, while the R11A and R22A enzymes exhibited ~34% and ~48% of wild-type activity, respectively. The saturation plots of the wild type compared to those of the R22A and R25A enzymes are shown in Figure 4A. Conversely, the R45A, R5A, and R33A enzymes displayed V_{max} values higher than that of the wild type: 1.4-, 1.7-, and 5.5-fold higher, respectively.

In the presence of F6P, all of the enzymes but R11A displayed somewhat higher $S_{0.5}$ values for ATP, ranging from 4-fold for the R25A enzyme to 12-fold for the R45A enzyme. This range is reflective of both the differences in the values in the absence of F6P and the inability of F6P to significantly increase the apparent affinity relative to its ~4-fold effect on the wild type. Similar trends were seen with the diminished effects of F6P on V_{max} for the enzymes except for R22A, R25A, and R32A. F6P completely restored the activity of the R22A enzyme (relative to the value seen in the absence of F6P) to wild-type levels as shown in both Table 2 and Figure 4B. Although the R25A enzyme displayed only ~1.6% of wild-type activity (see Table 2 and Figure 4B), this represents a significant increase compared to the activity measured in the absence of F6P. It should be noted that F6P had no effect on the kinetic parameters for

Table 2: Kinetic Parameters[a] for the Substrate ATP of ADPGlc PPase Arginine Mutants

	ATP		ATP with 2 mM F6P		ATP with 2 mM pyruvate	
enzyme	$S_{0.5}$ (mM) (Hill number)	V_{max} (units/mg)	$S_{0.5}$ (mM) (Hill number)	V_{max} (units/mg)	$S_{0.5}$ (mM) (Hill number)	V_{max} (units/mg)
WT	0.21 ± 0.04 (1.3 ± 0.2)	12.1 ± 1.0	0.051 ± 0.004 (1.3 ± 0.1)	147.9 ± 4.1	0.10 ± 0.01 (1.9 ± 0.3)	105 ± 5
R5A	0.49 ± 0.03 (1.3 ± 0.1)	20.20 ± 0.50	0.33 ± 0.01 (1.2 ± 0.1)	45.7 ± 1.0	0.29 ± 0.03 (1.5 ± 0.2)	22.9 ± 1.4
R11A	0.47 ± 0.1 (2.4 ± 0.5)	4.10 ± 0.50	0.05 ± 0.01 (1.5 ± 0.5)	8.3 ± 0.5	0.29 ± 0.02 (2.1 ± 0.4)	5.0 ± 0.3
R22A	0.71 ± 0.17 (1.0 ± 0.1)	5.80 ± 0.60	0.39 ± 0.06 (2.0 ± 0.4)	160.0 ± 12.0	0.35 ± 0.05 (1.2 ± 0.2)	33.0 ± 5.0
R25A	0.45 ± 0.05 (1.5 ± 0.2)	0.03 ± 0.002	0.20 ± 0.02 (1.3 ± 0.1)	2.3 ± 0.06	0.56 ± 0.04 (1.6 ± 0.2)	2.0 ± 0.1
R32A	0.20 ± 0.02 (2.1 ± 0.3)	11.60 ± 0.30	0.25 ± 0.02 (2.0 ± 0.2)	125.1 ± 3.9	0.39 ± 0.03 (1.7 ± 0.2)	98.6 ± 2.6
R33A	0.44 ± 0.07 (1.3 ± 0.2)	66.3 ± 5.0	0.43 ± 0.10 (1.3 ± 0.3)	62.0 ± 8.0	0.07 ± 0.01 (1.7 ± 0.2)	115.6 ± 6.0
R45A	0.60 ± 0.03 (2.2 ± 0.3)	17.0 ± 3.0	0.63 ± 0.04 (1.9 ± 0.2)	17.2 ± 2.0	0.60 ± 0.03 (2.0 ± 0.2)	40.0 ± 5.0

[a] Experiments for constructing saturation plots were performed in the presence of 5 mM Mg^{2+} and 1 mM Glc-1-P under standard conditions as described in Experimental Procedures.

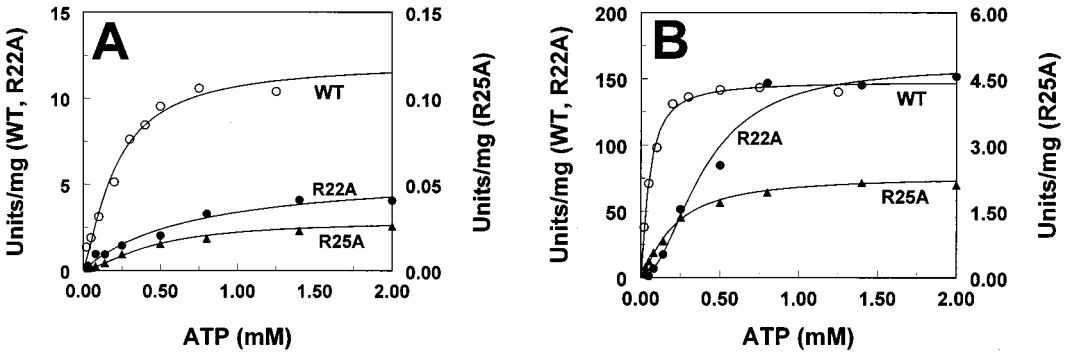

FIGURE 4: ATP saturation plots for wild-type (WT) and the R22A and R25A mutant ADPGlc PPases performed in the absence of activator (A) and in the presence of 2 mM F6P (B). See Experimental Procedures for details.

Table 3: Activation Kinetics[a] of *A Tumefaciens* ADPGlc PPase Arginine Mutants

	F6P			pyruvate			
enzyme	$A_{0.5}$(F6P) (mM) (Hill number)	V_{mA}(F6P) (units/mg)	activation(F6P)[b] (*x*-fold)	$A_{0.5}$(Pyr) (mM) (Hill number)	V_{mA}(Pyr) (units/mg)	activation(Pyr) (*x*-fold)	activation ratio[c] (F6P/Pyr)
WT	0.13 ± 0.01 (2.0 ± 0.3)	145 ± 5	12	0.10 ± 0.01 (1.9 ± 0.3)	102 ± 5	8.5	1.4
R5A	0.17 ± 0.09 (1 ± 0.4)	53 ± 7	3	na[d]	23 ± 5	1	3
R11A	0.03 ± 0.008 (1.3 ± 0.4)	7.2 ± 0.2	1.8	na[d]	5.0 ± 0.5	1	1.8
R22A	0.90 ± 0.05 (4.3 ± 1.0)	160 ± 10	27.6	0.15 ± 0.02 (1.5 ± 0.3)	35.1 ± 1.3	6.4	4.3
R25A	0.75 ± 0.04 (2.1 ± 0.2)	2.6 ± 0.2	91	0.18 ± 0.01 (2.5 ± 0.2)	1.97 ± 0.03	66	1.3
R32A	1.49 ± 0.08 (1.9 ± 0.2)	139 ± 4	12.4	0.12 ± 0.01 (1.8 ± 0.2)	100.6 ± 1.9	8.5	1.5
R33A	na[d]	60 ± 6	1	0.02 ± 0.005 (1.8 ± 0.2)	120.0 ± 4.0	2	0.5
R45A	na[d]	17.2 ± 3.1	1	0.69 ± 0.09 (2.4 ± 0.6)	40.9 ± 1.9	2.4	0.4

[a] Experiments for constructing saturation plots were performed in the presence of 2 mM ATP, 5 mM Mg^{2+}, and 1 mM Glc-1-P under standard conditions as described in Experimental Procedures. [b] The level of activation is defined as the velocity in the presence of saturating F6P (V_A) divided by the velocity in the absence of activator (V_O) (V_A/V_O). [c] The activation ratio is defined as the ratio of the level of F6P activation divided by the level of pyruvate activation. [d] No significant activation.

R33A and R45A. The range of $S_{0.5}$ and V_{max} values shown in the presence of pyruvate (compared to the wild-type values) is similar to the ranges in the presence of F6P. Interestingly, the extreme N-terminus R5A and R11A enzymes, which were activated in the presence of F6P, showed little response to pyruvate beyond a modest effect on the $S_{0.5}$ value for ATP. Conversely, the F6P insensitive R33A and R45A enzymes were activated by pyruvate. The effect of pyruvate on the R45A enzyme was solely as a V-type activator. In addition to an apparent V_{max} effect, pyruvate significantly lowered the ATP $S_{0.5}$ value for the R33A enzyme. The R11A enzyme exhibits opposite behavior in that F6P significantly lowers the ATP $S_{0.5}$ value while also increasing the apparent V_{max}.

Effect of Mutations on Regulatory Properties. As a number of the substituted ADPGlc PPases demonstrated altered regulatory properties in comparison with those of the wild type, it was of interest to analyze the effects of the mutations on the kinetics of activation by F6P and pyruvate. Table 3 displays the kinetic parameters and levels of activation for F6P and pyruvate as well as the ratios of activation by F6P to pyruvate (activation ratio).

The extreme N-terminus R5A and R11A enzymes displayed apparent affinities for F6P in the same range as that of the wild type but reduced levels of activation and apparent V_{max} values. These substituted enzymes were completely insensitive to pyruvate, consistent with the ATP saturation plots in the presence of pyruvate (Table 2). The higher observed activation ratios for these enzymes compared to that of the wild type reflect the diminution of the effects of pyruvate relative to F6P. Figure 5 displays the effects of F6P (A) and pyruvate (B) on the R5A enzyme in comparison to wild-type and other altered enzymes.

The R22A, R25A, and R32A enzymes displayed $A_{0.5}$ values for F6P that were 6.9-, 5.8-, and 11.5-fold higher than that of the wild type. The close agreement between the R32A

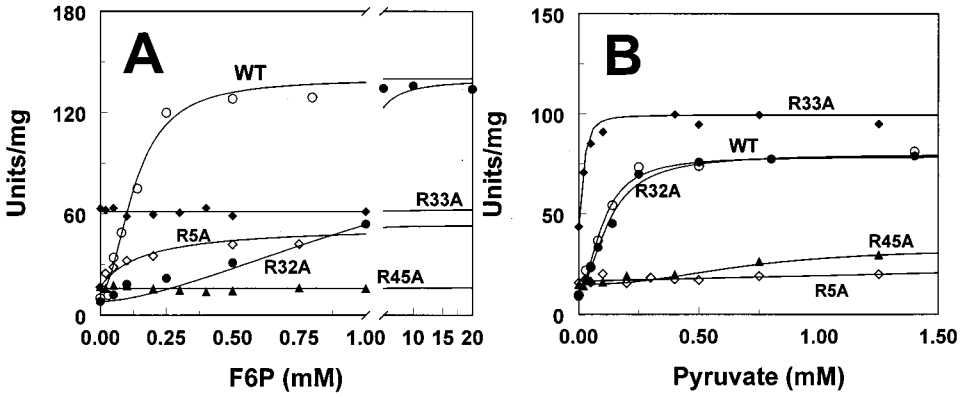

FIGURE 5: Effect of F6P (A) and pyruvate (B) on the wild-type (WT) and R5A, R32A, R33A, and R45A mutant ADPGlc PPases. Saturation plots were constructed as described in Experimental Procedures.

and wild-type enzymes in the levels of activation by F6P and the kinetic parameters for pyruvate activation is clearly shown in panels A and B of Figure 5, indicating that the only significant effect of this mutation is on F6P affinity. The R22A and R25A enzymes also exhibited 2.3- and 7.6-fold increased levels of activation by F6P relative to that of the wild type. In fair agreement with the ATP saturation data listed in Table 2, the V_{max} for the R22A enzyme was essentially identical to that of the wild type, while the R25A enzyme value was only ~1.6% of that of the wild type. The R22A and R25A enzymes displayed $A_{0.5}$ values for pyruvate in fair agreement with that of the wild type. The R22A enzyme exhibited a level of activation moderately lower than that of the wild type, and the R25A enzyme displayed a level of activation by pyruvate increased 7.8-fold relative to that of the wild type. The activation ratio for the R22A enzyme reflects an increased sensitivity to F6P relative to pyruvate. In the case of the R25A enzyme, the nearly identical increased levels of activation by both F6P and pyruvate resulted in an activation ratio very close to that of the wild type.

The R33A and R45A enzymes were completely insensitive to F6P as shown in Figure 5A, in agreement with the data listed in Tables 2 and 3. Given that the F6P-stimulated activity of the wild-type enzyme was the most sensitive to PGO modification (Figures 2 and 3), it was of interest to determine the response of these F6P insensitive enzymes to chemical modification. These altered enzymes were insensitive to PGO as shown in Figure 6. Taken together with the protection data (Figure 3), these results indicate a relationship between R33 and R45 in F6P binding and effect. The R33A enzyme exhibited a 5-fold lower $A_{0.5}$ value for pyruvate, while the R45A enzyme showed a ~7-fold increase in its $A_{0.5}$ value. Both of these enzymes exhibited significantly lower levels of activation by pyruvate compared to that of the wild type. The lower activation ratios for these enzymes compared to that of the wild type reflect the decreased effect of F6P relative to pyruvate.

The effects of the mutations on P_i inhibition in the absence of any other effectors were also preliminarily examined. As previously indicated, the wild-type enzyme was found to be 50% inhibited by 1 mM P_i. The R5A and R11A enzymes were more sensitive to P_i inhibition than the wild type (showing 78% and 67% inhibition, respectively); the R22A, R25A, and R32A enzymes were less sensitive to the inhibitor (displaying 20%, 33%, and 35% inhibition, respectively),

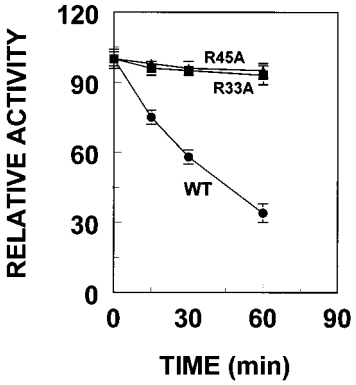

FIGURE 6: Effect of PGO (5 mM) modification on the activity of wild-type (WT), R33A, and R45A enzymes. The activity was measured in the presence of 2 mM F6P. The initial specific activities of the WT, R33A, and R45A enzymes were 147.9 ± 4.1, 62.0 ± 8.0, and 17.2 ± 2.0 units/mg, respectively.

while the R33A and R45A enzymes were completely insensitive to inhibition by 1 mM P_i.

DISCUSSION

Expression and Purification of Wild-Type and Altered Enzymes. This report establishes an efficient method for expressing and purifying large amounts of *A. tumefaciens* ADPGlc PPase to near homogeneity. This procedure resulted in the generation of ~175 units of pure enzyme per gram of induced cells compared to ~4 units per gram by the previous method (*19*). As has been recently shown with the *Rb. sphaeroides* ADPGlc PPase (*14*), the pSE420 vector, which includes a strong *trc* promoter and a translational enhancer and ribosome-binding site from gene 10 of bacteriophage T7, is clearly a very effective overexpression vector for ADPGlc PPase.

The only altered enzyme that was unable to be purified was R60A. The absence of activity in the R60A enzyme crude extract may reflect a lack of stability and/or disruption of protein folding that could lead to its rapid proteolysis (see Experimental Procedures). It is worth noting that a mutation at the analogous position in the *E. coli* ADPGlc PPase (from arginine to cysteine at position 67) was identified as being responsible for reduced stability as this altered enzyme was heat sensitive and lost activity when stored in the absence of 20% glycerol (*29*). The mutation also conferred reduced sensitivity to both activation by FBP and inhibition by AMP. Although the instability of this altered enzyme was hypoth-

esized to result from oxidation of the introduced cysteine, no supportive data were given nor, to our knowledge, were any other substitutions at this position analyzed.

Chemical Modification with PGO. Data from both the chemical modification and protection studies indicate the presence of populations of functional arginine residues residing in different subsites with different sensitivity and/or accessibility to PGO. The observed stimulation of the activity in the absence of F6P might be explained by PGO modification of an allosteric site partially mimicking the effect of the activator. The observed linear desensitization to F6P (Figure 2) clearly establishes a different subsite for F6P from pyruvate. The inactivation of the control rate by 10 mM PGO might be ascribed to modification of the active site.

The existence of specific but partially overlapping subsites containing arginines is further reinforced by the protection studies whose results are shown in Figure 3. F6P better protected F6P activation of the enzyme, while pyruvate more effectively protected pyruvate activation (Figure 3). The partial protection by the inhibitor P_i is indicative of binding of this anion at or near the allosteric subsite(s) for F6P and pyruvate resulting in inhibition. Such an interaction could be described by Segel's system A2 (*30*; inhibitor competitive with nonessential activator). Alternatively, P_i binding may result in a conformational change that renders the allosteric site less accessible. The same factors could explain the protection of allosteric properties by the substrate ATP. This protection by substrate was also recently observed for the *Rb. sphaeroides* ADPGlc PPase (*13*). Alanine scanning mutagenesis of the amino-terminal arginines has meaningfully extended the possible interpretation of this chemical modification data by providing the first evidence for distinct functional roles.

Effect of Arginine Mutations in the Glycine Rich Region. This study has provided experimental evidence for a role of arginines in the glycine rich region of ADPGlc PPase in both F6P activation and optimal catalysis. The inactivation observed by higher concentrations of PGO might correlate to modification of one or both of these arginine residues. Both the R22A and R25A altered enzymes exhibited reduced apparent affinities for F6P. A similar glycine rich region has been shown to be part of an FBP binding loop in *E. coli* glycerol kinase (*31*). Further, both the *Anabaena* PCC 7120 and the *B. stearothermophilus* ADPGlc PPases (see Figure 1) which are not activated by sugar phosphates have substitutions in the position analogous to R22. Interestingly, this same relative position in the potato ADPGlc PPase large subunit was shown to be important in interaction with the activator 3PGA: a mutation of glutamate 38 to lysine resulted in increased affinity for the activator (*32*). This led Greene et al. to postulate that the introduced positive charge could interact with the negatively charged activator. The R25A enzyme displays a low V_{max} value indicative of a role for this arginine in optimal catalysis. Arginine 25 may be near the catalytic site. The reduced affinity for activators, reduced activity, and reduced level of inhibition by P_i are also consistent with these mutations stabilizing a T state. The rather modest effects on the apparent ATP affinity probably reflect only a minor role for R25 in ATP binding. A similar observation has been reported recently for F6P 2-kinase (*33*). Significantly, recent data from the site-directed mutagenesis of the analogous arginine position to alanine in the *E. coli N*-acetylglucosamine-1-phosphate uridyltransferase (*34*; a distant member of the pyrophosphorylase superfamily) are generally consistent with our results. The uridyltransferase activity drastically decreased from 350 to 0.06 unit/mg, while the apparent affinity for UTP decreased only ~3-fold. The greater than 3 orders of magnitude diminution of V_{max} for this enzyme certainly indicates a more direct role for catalysis. Systematic mutagenesis of the glycine rich region in *A. tumefaciens* (see Figure 1, amino acids 18−23) is currently being carried out to obtain a more detailed understanding of its role.

Effect of Arginine Mutations on Regulatory Properties. The data from Table 3 and Figure 5 clearly establish diverse roles for the amino-terminal arginines in the regulation of *A. tumefaciens* ADPGlc PPase by F6P and/or pyruvate. The major effects of these mutations can be divided into three general groups: (1) desensitization to pyruvate (R5A and R11A enzymes), (2) decreased F6P affinity (R32A enzyme), and (3) desensitization to F6P (R33A and R45A enzymes).

The extreme N-terminal arginines 5 and 11 are quite clearly involved in activation by pyruvate, perhaps in part by providing an anionic binding site for the carboxyl group. The observed partial desensitization to F6P activation for these enzymes supports the hypothesis of partially overlapping binding sites for the activators (*13*). Perhaps one or both of these arginines could be protected by pyruvate, resulting in the data shown in Figure 3. More broadly, these results support the general importance of the less conserved extreme N-terminus in ADPGlc PPases in regulation. As previously mentioned, N-terminal proteolysis (the first 10−13 amino acids; *11*) and truncation mutagenesis (of the first 11 amino acids; *12*) of the *E. coli* enzyme resulted in desensitization to activation and inhibition.

The R32A enzyme displays a reduced apparent affinity for F6P that would be consistent with this arginine playing a role in facilitating optimal binding. The near-superimposable pyruvate saturation plots for the wild-type and R32A enzymes (Figure 5B) are further proof of separate subsites for these activators. The R32A enzyme is most similar in behavior to the partially purified *E. coli* K39E mutant ADPGlc PPase which displayed an $A_{0.5}$ for the activator FBP more than 20-fold higher than that of the wild type (*35*). Lysine 39 in the *E. coli* enzyme is analogous to arginine 32 in *A. tumefaciens* (see Figure 1). It should also be noted that bacterial ADPGlc PPases that are not activated by sugar phosphates, such as those from *Anabaena* PCC 7120 and *B. stearothermophilus*, have the nonconservative substitutions of leucine and asparagine, respectively, at this position. Further mutagenesis of this position is currently being carried out to determine the effects of size, charge, and hydrophobicity.

The R33 and R45 positions are clearly very important for activation by F6P. Both the R33A and R45A enzymes exhibit V_{max} values that are increased compared to that of the wild type in the absence of activator and are completely insensitive to F6P and 1 mM P_i. These substitutions appear to have resulted in the generation of enzymes locked into activated forms (R states) in the absence of F6P. This result is in accord with the PGO modification data in which the unactivated rate was increased concomitant with abolishment of the effects of F6P (which could be protected by F6P) and P_i

and partial desensitization to pyruvate. The R33 and/or R45 positions could well have been primary targets for PGO modification as reinforced by the data (Figure 6) showing that both the R33A and R45A enzymes were insensitive to PGO modification. The R33 position in particular has been predicted to be in an exposed loop (*2*) that could have been accessible to PGO modification.

The substitution of alanine at R33 leads to a dramatic increase in activity in the absence of F6P. It is possible that the substitution of the neutral alanine partially mimics the effect of charge neutralization in F6P binding to the wild-type ADPGlc PPase. As this arginine is adjacent to the R32 position that has been shown to be important for F6P affinity, it is tempting to speculate that R33 is the other major amino acid responsible for optimal F6P binding leading to activation. Specific arginine residues have been shown to be important in the binding of F6P to F6P 2-kinase: fructose 2,6-bisphosphatase (*36*) and pyrophosphate-dependent phosphofructokinase (*37*). Significantly, ADPGlc PPase variants that lack arginine at this position—the *Rs. rubrum* enzyme has a glutamate and the *B. stearothermophilus* enzyme an isoleucine (see Figure 1)—are insensitive to both sugar-phosphate activation and P_i inhibition.

As the R45 position is completely conserved across all ADPGlc PPase activator classes, it would seem to be unlikely to play a direct role in binding of a particular effector molecule. Rather, the R45 position may play a pivotal role (triggered by binding of effectors at a distant site) in the stabilization of a partially activated form of the enzyme.

Concluding Remarks. Taken together, chemical modification and site-directed mutagenesis data have established important and diverse functional roles for the N-terminal arginines of *A. tumefaciens* ADPGlc PPase. This study provides the foundation for future work aimed at elucidating the molecular mechanism of activation. In addition to functioning as part of anionic binding sites for effectors, some of these arginines (such as arginines 5, 22, 33, and 45) may play a role in stabilizing the T or R states of the enzyme as has been shown with fructose 1,6-bisphosphatase (*37*−*40*). Alternatively, substitution of some of these arginines could have triggered more indirect conformational changes resulting in the observed effects. The generation and analysis of mutant ADPGlc PPases with additional substitutions at these positions to probe the role of size, charge, polarity, and hydrophobicity are currently being carried out. The availability of other recombinant ADPGlc PPases such as those from *E. coli* (*11*), *Anabaena* PCC 7120 (*17*), and *Rb. sphaeroides* (*14*) opens up the possibility of the generation of various chimeric enzymes and altered chimeric enzymes for analysis. Ultimately, structural information will be required to fully understand the physical mechanism of activation. Toward this goal, our study has established a system for easily producing milligram quantities of pure protein for both wild-type and altered enzymes amenable to crystallization trials as a first step toward determining the three-dimensional structure of this enzyme.

ACKNOWLEDGMENT

We thank the Spring 1999 Advances in Biotechnology Laboratory class (Chemistry/Biological Science 472B) at California State University, Fullerton, for participating in the production, sequencing, and preliminary characterization of some of the site-directed mutants.

REFERENCES

1. Preiss, J. (1996) *Biotechnol. Annu. Rev. 2*, 259−279.
2. Preiss, J., and Sivak, M. N. (1998) *Genet. Eng. 20*, 177−223.
3. Preiss, J. (1996) in *Escherichia coli* and *Salmonella typhimurium: Cellular and Molecular Biology* (Neidhart, F. C., Ed.) 2nd ed., Vol. 1, pp 1015−1024, ASM Press, Washington, DC.
4. Preiss, J., and Romeo, T. (1989) *Adv. Microb. Physiol. 30*, 183−238.
5. Smith-White, B. J., and Preiss, J. (1992) *J. Mol. Evol. 34*, 449−464.
6. Monod, J., Wyman, J., and Changeux, J.-P. (1965) *J. Mol. Biol. 12*, 88−118.
7. Meyer, C. R., Bork, J. A., Nadler, S., Yirsa, J., and Preiss, J. (1998) *Arch. Biochem. Biophys. 353*, 152−159.
8. Greene, T. W., Chantler, S. E., Kahn, M. L., Barry, J. F., Preiss, J., and Okita, T. W. (1996) *Proc. Natl. Acad. Sci. U.S.A. 93*, 1509−1513.
9. Laughlin, M. J., Payne, J. W., and Okita, T. W. (1998) *Phytochemistry 47*, 621−629.
10. Meyer, C. R., Ghosh, P., Nadler, S., and Preiss, J. (1993) *Arch. Biochem. Biophys. 302*, 64−71.
11. Wu, M.-X., and Preiss, J. (1998) *Arch. Biochem. Biophys. 358*, 182−188.
12. Wu, M.-X., and Preiss, J. (2001) *Arch. Biochem. Biophys. 389*, 159−165.
13. Meyer, C. R., Borra, M., Igarashi, R., Lin, Y. S., and Springsteel, M. (1999) *Arch. Biochem. Biophys. 372*, 179−188.
14. Igarashi, R. Y., and Meyer, C. R. (2000) *Arch. Biochem. Biophys. 376*, 47−58.
15. Carlson, C. A., and Preiss, J. (1982) *Biochemistry 21*, 1929−1934.
16. Iglesias, A. A., Kakefuda, G., and Preiss, J. (1992) *J. Protein Chem. 11*, 119−128.
17. Sheng, J., and Preiss, J. (1997) *Biochemistry 36*, 13077−13084.
18. Ball, K. L., and Preiss, J. (1992) *J. Protein Chem. 11*, 231−238.
19. Uttaro, A. D., Ugalde, R. A., Preiss, J., and Iglesias, A. A. (1998) *Arch. Biochem. Biophys. 357*, 13−21.
20. Eidels, I., Edelmann, P. L., and Preiss, J. (1970) *Arch. Biochem. Biophys. 140*, 60−74.
21. Takata, H., Takaha, T., Okada, S., Takagi, M., and Imanaka, T. (1997) *J. Bacteriol. 179*, 4689−4698.
22. Thompson, J. D., Higgins, D. G., and Gibson, T. J. (1994) *Nucleic Acids Res. 22*, 4673−4680.
23. Bradford, M. (1976) *Anal. Biochem. 72*, 248−254.
24. Laemmli, U. K. (1970) *Nature 227*, 680−685.
25. Ghosh, H. P., and Preiss, J. (1966) *J. Biol. Chem. 241*, 4491−4505.
26. Preiss, J., Shen, L., Greenberg, E., and Gentner, N. (1966) *Biochemistry 5*, 1833−1845.
27. Brooks, S. P. J. (1992) *BioTechniques 13*, 906−911.
28. Brosius, J., and Holy, A. (1984) *Proc. Natl. Acad. Sci. U.S.A. 81*, 6929−6933.
29. Ghosh, P., Meyer, C., Remy, E., Peterson, D., and Preiss, J. (1992) *Arch. Biochem. Biophys. 296*, 122−128.
30. Segel, I. H. (1975) *Enzyme Kinetics, Behavior and Analysis of Rapid Equilibrium and Steady-State Enzyme Systems*, John Wiley & Sons, New York.
31. Ormo, M., Bystrom, C. E., and Remington, S. J. (1998) *Biochemistry 37*, 16565−16572.
32. Greene, T. W., Kavakli, I. H., Kahn, M. L., and Okita, T. W. (1998) *Proc. Natl. Acad. Sci. U.S.A. 95*, 10322−10327.
33. Mizuguchi, H., Cook, P. F., Hasemann, C. A., and Uyeda, K. (1997) *Biochemistry 36*, 8775−8784.
34. Brown, K., Pompeo, F., Dixon, S., Mengin-Lecreulx, D., Cambillau, C., and Bourne, Y. (1999) *EMBO J. 18* (15), 4096−4107.
35. Gardiol, A., and Preiss, J. (1990) *Arch. Biochem. Biophys. 280*, 175−180.

36. Uyeda, K., Wang, X.-L., Mizugchi, H., Li, Y., Nguyen, C., and Hasemann, C. A. (1997) *J. Biol. Chem. 272*, 7867−7872.
37. Deng, Z., Wang, X., and Kemp, R. G. (2000) *Arch. Biochem. Biophys. 380*, 56−62.
38. Lu, G., Williams, M. K., Giroux, E. L., and Kantrowitz, E. R. (1995) *Biochemistry 34*, 13272−13277.
39. Giroux, E., Williams, M. K., and Kantrowitz, E. R. (1994) *J. Biol. Chem. 269*, 31404−31409.
40. Shyur, L.-F., Poland, B. W., Honzatko, R. B., and Fromm, H. J. (1997) *J. Biol. Chem. 272*, 26295−26299.

BI002615E